Anal Bioanal Chem (2007) 387:277–285
DOI 10.1007/s00216-006-0930-3

ORIGINAL PAPER

A microfluidic system for evaluation of antioxidant capacity based on a peroxyoxalate chemiluminescence assay

Maliwan Amatatongchai · Oliver Hofmann · Duangjai Nacapricha · Orawon Chailapakul · Andrew J. deMello

Received: 1 September 2006 / Revised: 9 October 2006 / Accepted: 11 October 2006 / Published online: 28 November 2006

Abstract A microfluidic system incorporating chemiluminescence detection is reported as a new tool for measuring antioxidant capacity. The detection is based on a peroxyoxalate chemiluminescence (PO-CL) assay with 9,10-bis-(phenylethynyl)anthracene (BPEA) as the fluorescent probe and hydrogen peroxide as the oxidant. Antioxidant plugs injected into the hydrogen peroxide stream result in inhibition of the CL emission which can be quantified and correlated with antioxidant capacity. The PO-CL assay is performed in 800-μm-wide and 800-μm-deep microchannels on a poly(dimethylsiloxane) (PDMS) microchip. Controlled injection of the antioxidant plugs is performed through an injection valve. Of the plant-food based antioxidants tested, β-carotene was found to be the most efficient hydrogen peroxide scavenger (SA_{HP} of 3.27×10^{-3} μmol^{-1} L), followed by α-tocopherol (SA_{HP} of 2.36×10^{-3} μmol^{-1} L) and quercetin (SA_{HP} of 0.31×10^{-3} μmol^{-1} L). Although the method is inherently simple and rapid, excellent analytical performance is afforded in terms of sensitivity, dynamic range, and precision, with RSD values typically below 1.5%. We expect our microfluidic devices to be used for in-the-field antioxidant capacity screening of plant-sourced food and pharmaceutical supplements.

Keywords Antioxidant capacity · Peroxyoxalate chemiluminescence · Microfluidics

M. Amatatongchai · D. Nacapricha
Department of Chemistry, Faculty of Science, Mahidol University, 10400 Bangkok, Thailand

M. Amatatongchai
Department of Chemistry, Faculty of Science, Ubonrajathanee University, 34190 Ubonratchathani, Thailand

O. Hofmann
BioIncubator Unit, Bessemer Building (RSM) Level 1, Prince Consort Road, London SW7 2BP, UK

O. Chailapakul
Department of Chemistry, Faculty of Science, Chulalongkorn University, 10330 Bangkok, Thailand

A. J. deMello (✉)
Department of Chemistry, Imperial College London, London SW7 2AZ, UK
e-mail: a.demello@imperial.ac.uk

Introduction

In response to both external and internal stimuli, small amounts of reactive oxygen species (ROS) are constantly generated within aerobic organisms. These ROS species include hydrogen peroxide (H_2O_2) and the hydroxyl ($HO^{\bullet}$) and superoxide ($O_2^{-\bullet}$) radicals. In healthy individuals production of ROS is balanced by the antioxidative defence system. In situations in which there is a serious imbalance between production of ROS and antioxidative defence, cell injury occurs. This situation is normally defined as "oxidative stress" which results in damage to DNA, proteins, lipids, and uric acid. Oxidative stress is often found in patients suffering from chronic conditions such as Alzheimer's and Parkinson's disease. Damage caused by the action of free radicals may, moreover, initiate and promote the progression of several chronic diseases, for example cancer, cardiovascular disease, and inflammation [1]. Under conditions of oxidative stress, production of the free radicals is favoured, which results in reduction of antioxidant levels.

The benefit of dietary intake of antioxidant compounds, either as food additives or as pharmaceutical supplements, in protecting the body against oxidative stress has been

widely recognized. Antioxidant compounds, for example phenolic acids, polyphenols, and flavonoids, scavenge free radicals such as peroxide and superoxide, thereby inhibiting the oxidative mechanism [2]. Primary sources of naturally occurring antioxidants are whole grain, fruit, and vegetables. Plant-sourced food antioxidants, for example vitamin C, vitamin E, carotenes, and phenolic acids, have also been shown to scavenge ROS [3].

Over the past few years there has been significant interest in developing new methods for assessing total antioxidant capacity (TAC) in medicinal plant extracts and biological fluids. A variety of tests has been developed, including colorimetric [4–7], fluorimetric [8, 9], electrochemical [10], and chromatographic assays [11]. Of particular interest are chemiluminescence based tests which offer a simple but sensitive means of monitoring low antioxidant levels [12–15]. Because the chemical reaction acts as an internal source of light, instrumental requirements and background noise levels are low. Some studies have assessed antioxidant scavenging capacity by means of direct chemiluminescence (CL) assays based on luminol oxidation catalyzed by horseradish peroxidase [16, 17]. In such studies, light emission is suppressed when antioxidants are present. Although these methods are accurate, use of an enzyme extends analysis times and reactions are prone to interference from other sample constituents.

Arnous et al. [18] and Mansouri and co-workers [19] recently proposed a cuvette-based method for evaluation of scavenging of hydrogen peroxide by natural and polyphenolic antioxidants, using indirect peroxyoxalate chemiluminescence (PO-CL) and 9,10-diphenylanthracene (DPA) as a fluorescent probe. PO-CL was first reported in 1963 by Chandross [20] who observed that when oxalyl chloride reacts with hydrogen peroxide in the presence of a fluorophore such as DPA high intensity, short-lived, blue emission is observed. The reaction comprises three basic steps (Scheme 1) [21–23]. In the first step, an aryl oxalate ester, for example bis(2,4,6-trichlorophenyl)oxalate (TCPO), reacts with hydrogen peroxide to produce the key intermediate, C_2O_4, which provides the necessary excitation energy. The second step involves chemically induced excitation of a fluorophore to a vibronic excited state. The final step is excited state deactivation by emission of radiation. Rauhut and co-workers successfully adapted the PO-CL reaction to a variety of fluorophores [24, 25].

From the above mechanism it is evident that H_2O_2 is essential for CL generation and, therefore, that its removal leads to CL inhibition. When an antioxidant is present in the assay mixture it scavenges the hydrogen peroxide and quenches the production of light. By use of a constant amount of peroxyoxalate and hydrogen peroxide the activity of antioxidants can thus be determined from the decrease in chemiluminescence emission. PO-CL-based determination of hydrogen peroxide scavenging activity can be performed by plotting I_0/I against antioxidant concentration (C), where I_0 and I are the emission intensities before and after addition of antioxidant, respectively:

$$I_0/I = aC + b \tag{1}$$

where a and b represent the gradient and y-intercept, respectively. By setting $I_0/I=2$, the amount of each antioxidant required to induce a 50% reduction in emission intensity (IC_{50}) can be calculated. The scavenging activity (SA_{HP}), for hydrogen peroxide in this case, is defined as:

$$SA_{HP} = 1/IC_{50} \tag{2}$$

In this paper we report a novel microfluidic method for estimating total antioxidant-scavenging capacity based on a modified PO-CL assay with 9,10-bis-(phenylethynyl)anthracene (BPEA) as the fluorophore. BPEA is commonly used in green lightsticks but has not previously been applied to antioxidant assays. It has a high quantum yield and the green emission is well matched to the responsivity of our organic photodetectors which we intend to use in

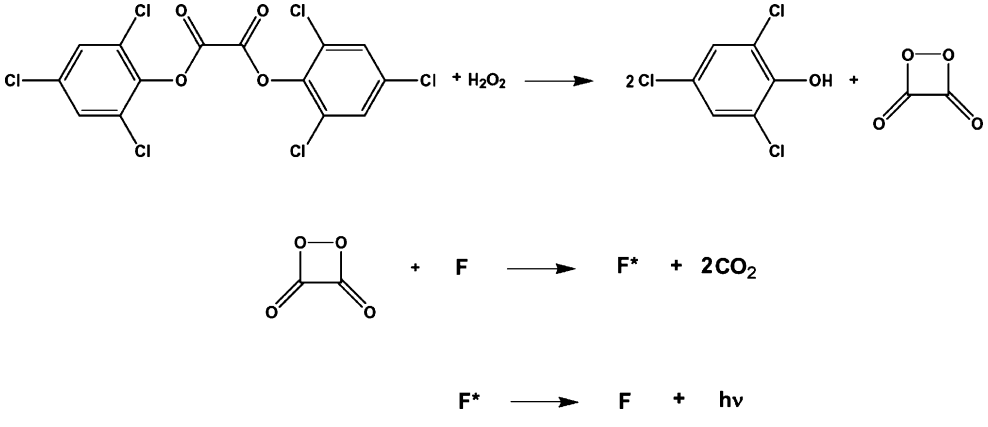

Scheme 1 Schematic diagram of the PO-CL reaction mechanism

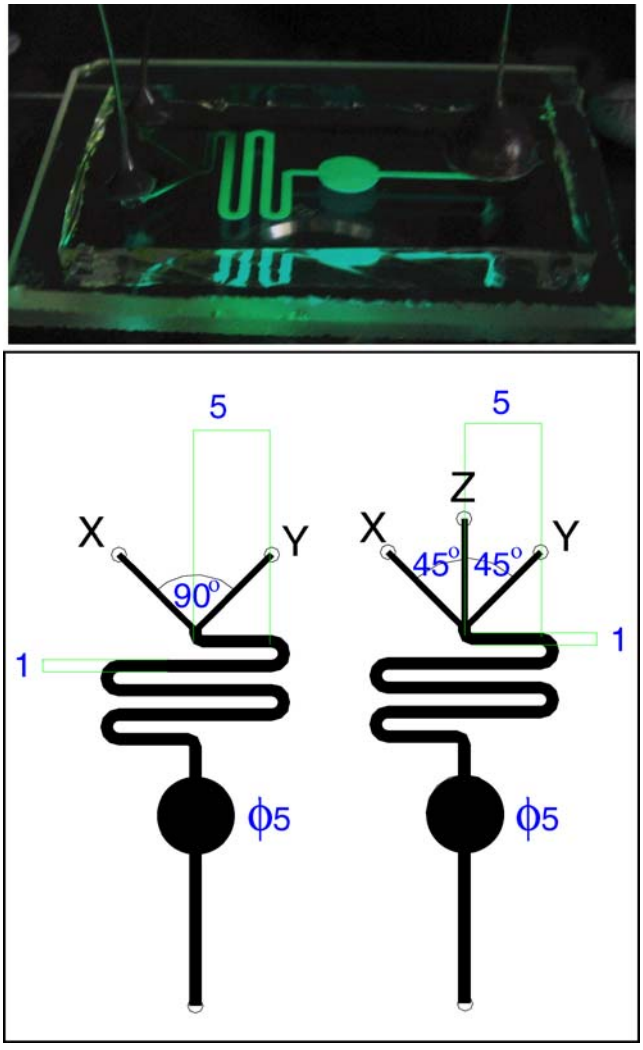

Fig. 1 Schematic diagram of the two-inlet (*left*) and three-inlet (*right*) PDMS microchips used. The microfluidic circuit comprises the inlets, a 800-μm-wide and 800-μm-deep mixing channel and a 5-mm-wide and 800-μm-deep circular detection chamber. Inlets *X*, *Y*, and *Z* were connected to the reagent, dye, and catalyst mixture, hydrogen peroxide, and antioxidant solution, respectively, and the outlet was connected to waste. The *photograph* depicts an assembled PDMS microchip sandwiched between two glass plates with the top plate containing capillary reservoirs. Please note the CL emission generated in the mixing channel downstream of the point of confluence of the reagent, dye, and catalyst mixture and the hydrogen peroxide

portable antioxidant capacity screening devices. Here we use a microfluidic format for diffusion-based mixing of PO-CL reagents and controlled injection of antioxidant plugs. In recent years, microfluidic devices have been used in a variety of applications including molecular biology, small-molecule organic synthesis, immunoassays, and cell manipulation [26]. Such systems have been shown to have significant advantages over their macroscale analogues, including improved efficiency with regard to reagent consumption, response times, analytical performance, integration, system control, and throughput [27–29]. In this work we have used these advantages to create a microfluidic system that enables rapid and automated determination of total antioxidant capacity using minute volumes of reagent and antioxidant.

Experimental

Microfluidic device fabrication

Our CL microfluidic devices were fabricated in-house as described in detail elsewhere [30, 31]. In brief, we used a fast prototyping approach based on soft lithography. First a master was fabricated by illuminating an SU-8 coated glass substrate through a photomask comprising the microchannel layout. After development this resulted in a master with a positive surface structure. The microfluidic layer was then fabricated by moulding with poly(dimethylsiloxane) (PDMS). To form the structured PDMS layer, PDMS base and curing agent (Sylgard 184; Dow Corning, Wiesbaden, Germany) were mixed at a ratio of 10:1 (*w*/*w*), degassed and decanted on to the SU-8 master. After thermal curing at 95 °C for 1 h, the polymer layer was pealed off the master and sealed between two glass plates. The top plate contained access holes, coinciding with the microchannel ends, into which capillaries were inserted to serve as fluid reservoirs. Permanent bonding of this hybrid microchip was achieved by exposing the PDMS layer to an oxygen plasma for 30 s before microchip assembly (Plasma Prep II; Structure Probe, West Chester, USA). This yielded a robust microchip with no fluid leakage even at high flow rates and after extended use. Schematic diagrams of the layout of the fabricated microchannel patterns are shown in Fig. 1.

Reagents

For initial flow optimisation experiments all PO-CL reagents were extracted from OmniGlow green lightsticks (Omniglow, Salisbury, Wiltshire, UK). For all other antioxidant assay optimisation experiments bis(2-carbopentyloxy-3,5,6-trichlorophenyl) oxalate (CCPO), 9,10-bis (phenylethynyl)anthracene (BPEA), sodium salicylate, imidazole, 4-dimethylaminopyridine (DMAP), 31% hydrogen peroxide stock solution, ethyl acetate, and acetonitrile were purchased from Sigma–Aldrich (UK) and used as received. Antioxidant standards β-carotene (vitamin A), α-tocopherol (vitamin E), and quercetin were dissolved in 3:7 (*v*/*v*) ethyl acetate–acetonitrile and hydrogen peroxide was diluted with acetonitrile. For the on-chip antioxidant assay 100 μmol L^{-1} CPPO (PO-CL reagent), 1 mmol L^{-1} BPEA (dye), 100 μmol L^{-1} hydrogen peroxide (oxidant), and 2 mmol L^{-1} sodium salicylate (catalyst) were used.

Bulk chemiluminescence measurements

For catalyst optimisation experiments 1.8 mL BPEA (0.5 mmol L^{-1}) was mixed in a standard 1-cm path-length cuvette with 0.025 mL H_2O_2 (2.25 mmol L^{-1}) and 0.2 mL catalyst solution (4.5 mmol L^{-1}). CCPO solution (0.45 mmol L^{-1}, 0.2 mL) was then added and after mixing for 5 s the emission intensity was measured in a Fluoromax 2 system (Horiba Jobin Yvon, Stanmore, UK). For bulk antioxidant assays the following procedure was used. First, 1.8 mL BPEA (0.5 mmol L^{-1}) was mixed with 0.025 mL H_2O_2 (2.25 mmol L^{-1}) and 0.2 mL sodium salicylate catalyst (4.5 mmol L^{-1}). This reagent was called Mixture A. CCPO solution (0.45 mmol L^{-1}, 0.2 mL) and 0.05 mL antioxidant standard were then pipetted into a 1-cm path length cuvette and Mixture A was added, followed by manual mixing for 5 s. Chemiluminescence spectra from the reaction were then recorded continuously until a plateau was reached. Intensity values were measured after ~50 s, corresponding to peak emission. I_0 was measured from the water reference and I values were measured for the respective antioxidant standard additions.

Microfluidic system operation

Fluids were motivated through the microchannel network by use of a precision syringe pump (PHD 2000; Harvard Apparatus, Kent, UK). The empty microfluidic device was first filled with ethanol by capillary action. This process was crucial to efficient operation and enabled subsequent solutions to be reproducibly introduced into the hydrophobic PDMS channels. For the three-inlet microchip the mixture of PO-CL reagent, dye, and catalyst was pumped through inlet X, and antioxidant standards and hydrogen peroxide were introduced through inlets Z and Y, respectively (Fig. 1). For the two-inlet microchip the mixture of PO-CL reagent, dye, and catalyst was again pumped through the first inlet. In this configuration, however, hydrogen peroxide was introduced through the second inlet, with antioxidant plugs being injected into the hydrogen peroxide stream through an in-line Rheodyne valve with a 50 μL injection loop.

Detection system

Chemiluminescence emission was detected by use of an inverted fluorescence microscope equipped with a photomultiplier tube. Briefly, emission was collected by a microscope objective (10×, 0.42 NA; Newport, Irvine, CA, USA), and passed through the dichroic mirror, a suppression filter, and, finally, through an adjustable detection window. A photomultiplier tube (MEA153; Seefelder Messtechnik, Germany) functioning in current mode was used to detect fluorescence photons.

Results and discussion

Chemiluminescence is generated by the reaction of 2-carbopentyloxy-3,5,6-trichlorophenyl oxalate (CCPO) with hydrogen peroxide in the presence of the fluorophore BPEA and catalyst. All solutions were prepared in 3:7 (*v*/*v*) ethyl acetate–acetronitile. Bulk spectra of emission originating from the reaction of CCPO, BPEA, and hydrogen peroxide in the presence of three different catalysts are depicted in Fig. 2. Peak emission is always observed at 500 nm with maximum time-integrated intensity being obtained within ~50 s of reagent introduction. Maximum steady-state signals were obtained with 2 mmol L^{-1} sodium salicylate. These optimised conditions were used in subsequent experiments to evaluate the effect of antioxidants on CL intensity. For all antioxidants tested (β-carotene, α-tocopherol, and quercetin), emission intensity decreased as a function of antioxidant concentration. Figure 3 shows CL emission as a function of time for different concentrations of α-tocopherol (vitamin E) and the inset depicts the corresponding plot of I_0/I against concentration. As expected, linear dependency was observed for α-tocopherol and for all the other antioxidants.

Figure 4 shows CL signal traces obtained using the three-inlet microchip. In these experiments the mixture of PO-CL reagent, dye, and catalyst was delivered through inlet X and hydrogen peroxide through inlet Y, at volumetric flow rates of 40 μL min^{-1}, followed by addition of β-carotene (vitamin A) antioxidant standards through inlet Z at a volumetric flow rate of 40 μL min^{-1}. As shown in Fig. 4 an initial signal increase is observed approximate-

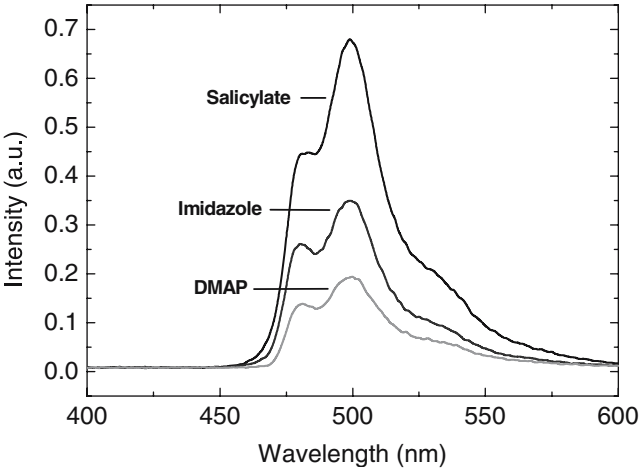

Fig. 2 Chemiluminescence spectra obtained from reaction of 1 mmol L^{-1} CCPO, 1 mmol L^{-1} BPEA, and 0.1 mmol L^{-1} hydrogen peroxide, in 3:7 (*v*/*v*) ethyl acetate–acetonitrile, with 2 mmol L^{-1} added catalysts sodium salicylate, imidazole, or 4-dimethylaminopyridine (DMAP)

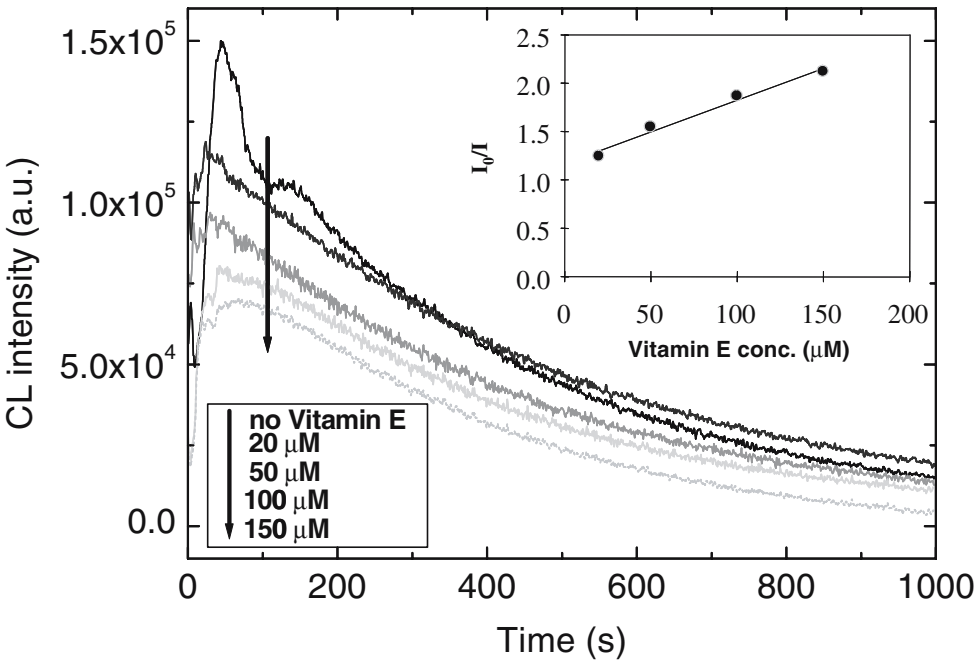

Fig. 3 CL intensity as a function of time for reaction of different concentrations of antioxidant α-tocopherol (vitamin E) with 0.1 mmol L^{-1} CCPO, 1 mmol L^{-1} BPEA, 0.1 mmol L^{-1} hydrogen peroxide, and 2 mmol L^{-1} sodium salicylate in 3:7 (*v*/*v*) ethyl acetate–acetonitrile. α-Tocopherol concentrations were 0, 20, 50, 100, and 150 μmol L^{-1}. The *inset* shows the relationship between I_0/I and α-tocopherol concentration

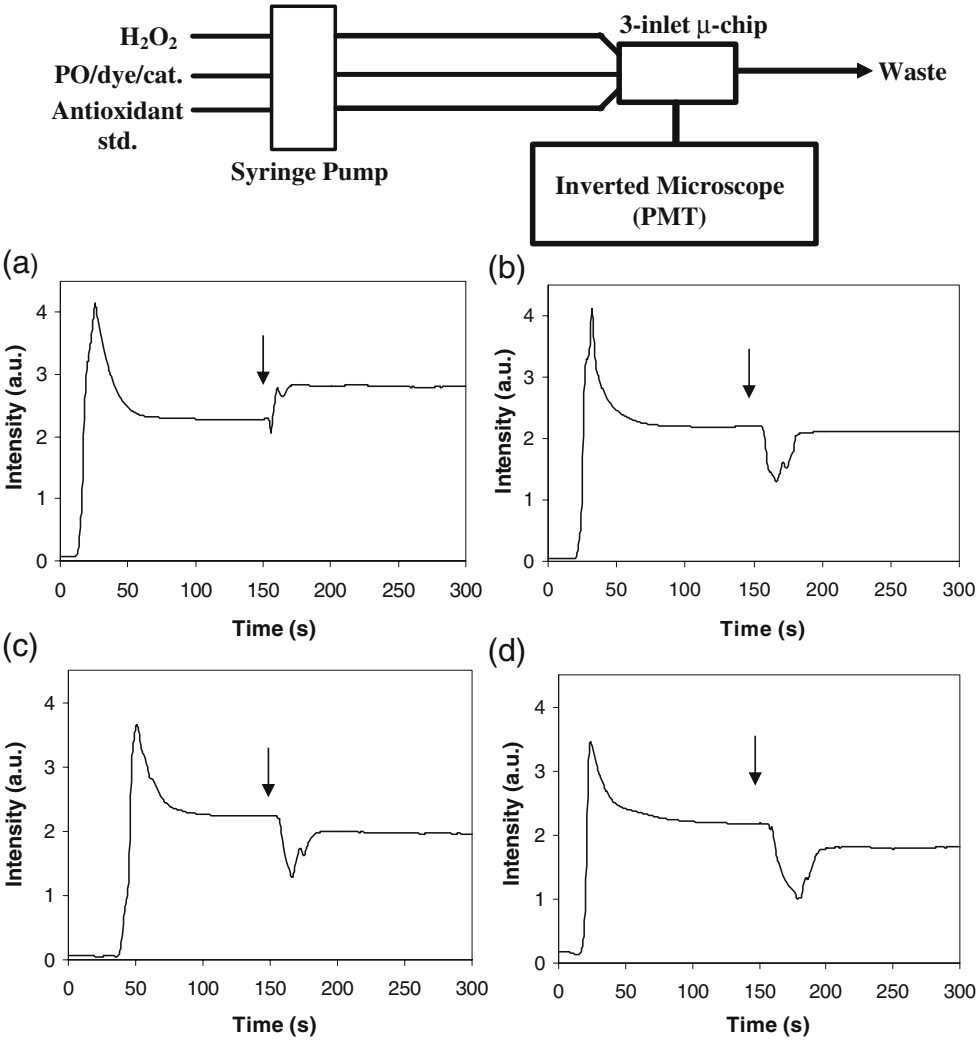

Fig. 4 Examples of the PMT signal profiles obtained from the three-inlet microchip. The profiles are for solutions containing 0 mmol L^{-1} (**a**), 5 mmol L^{-1} (**b**), 25 mmol L^{-1} (**c**), and 100 mmol L^{-1} (**d**) β-carotene. *Arrows* mark the time when the β-carotene flow was started through microchip inlet Z

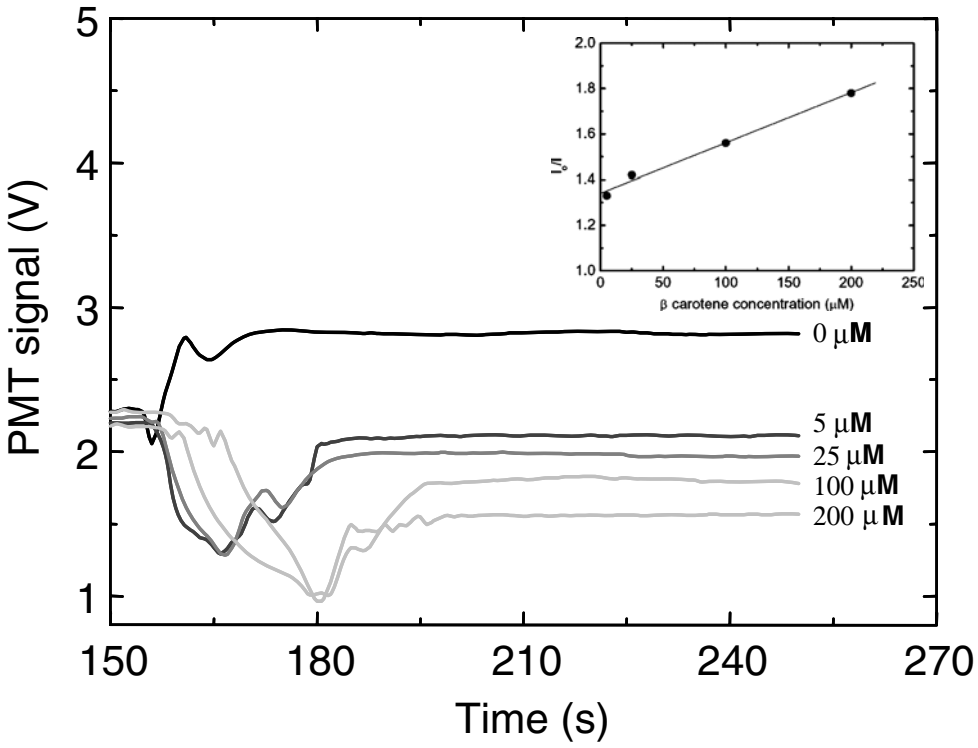

Fig. 5 Comparison of the PMT signal profiles obtained from the three-inlet microchip. For clarity the results from Fig. 4 were replotted with the starting time corresponding to the introduction of the antioxidant flow at ~150 s. The *inset* shows the relationship between I_0/I calculated from the plateau intensities for different β-carotene concentrations

ly 20 s after application of flow and reaches a maximum at 25–40 s. This is followed by a decrease in the signal and formation of a plateau after ~100 s. The signal profile differs substantially from those presented in Fig. 3 for bulk measurements. The microchip results are consistent with previously published data from our group and are indicative of diffusion-based mixing with a parabolic flow front [31]. After plateau formation the antioxidants are introduced and the expected decrease in CL emission is observed. Inspection of the CL traces reveals a signal decrease that is proportional to antioxidant concentration. This is shown in Fig. 5, in which a linear plot of I_0/I against antioxidant concentration is obtained. Interestingly the *y*-intercept deviates from unity which is consistent with previously published peroxyoxalate quenching data [18, 32]. We attribute this deviation to interfacial phenomena between the reagent flows [33].

The advantages of the microfluidic platform were subsequently exploited in a simple 2-inlet microchip with an in-line Rheodyne injection valve (50 μL injection loop) connected to the second inlet. The mixture of peroxyoxalate, dye, and catalyst was introduced through inlet X and hydrogen peroxide solution, with the injected antioxidant plugs, was introduced through inlet Y. Representative signal profiles obtained from multiple injection of α-tocopherol antioxidant plugs are displayed in Fig. 6. Close inspection of the temporal intensity variation shows the expected decrease in CL signal corresponding to the injected antioxidant volume but, interestingly, also reveals positive deviations before and after this signal decrease. For applied flow rates of 80 μL min^{-1} (total flow rate 160 μL min^{-1}) an average reagent residence time in the mixing channel of ~12 s can be calculated. For antioxidant molecules this equates to an average diffusion distance of 200 μm, or approximately one fourth of the width of the microchannel. This results in limited lateral mixing of the antioxidant plug with the adjacent stream of mixed peroxyoxalate, dye, and catalyst. CL emission occurs at the front and back of the plug only, where hydrogen peroxide is also present, partially scavenged by the diffusing antioxidant. Presumably the observed CL emission enhancement is due to stacking effects at the antioxidant plug–hydrogen peroxide interfaces resulting from solubility and density gradients induced by the different solvents used [34]. Antioxidant capacity was quantified by analysis of the first positive peak of each injection, as shown in Fig. 7. It is apparent that excellent linearity is obtained over the entire range of antioxidant concentration, 0–200 μmol L^{-1}.

It should be noted that these proof-of-concept experiments were chosen to demonstrate the validity, accuracy, and high reproducibility of our microfluidics-based method for determination of antioxidant capacity. Reduction of the dimensions of the microchannel and of the volume of the injected antioxidant plug, in conjunction with parallel operation, would afford significantly faster analysis and increased throughput to rival microtitre plate methods which are often hampered by poor mixing. Interestingly, there are similarities between our microchip-based method and flow injection analysis (FIA) in that a plug is injected

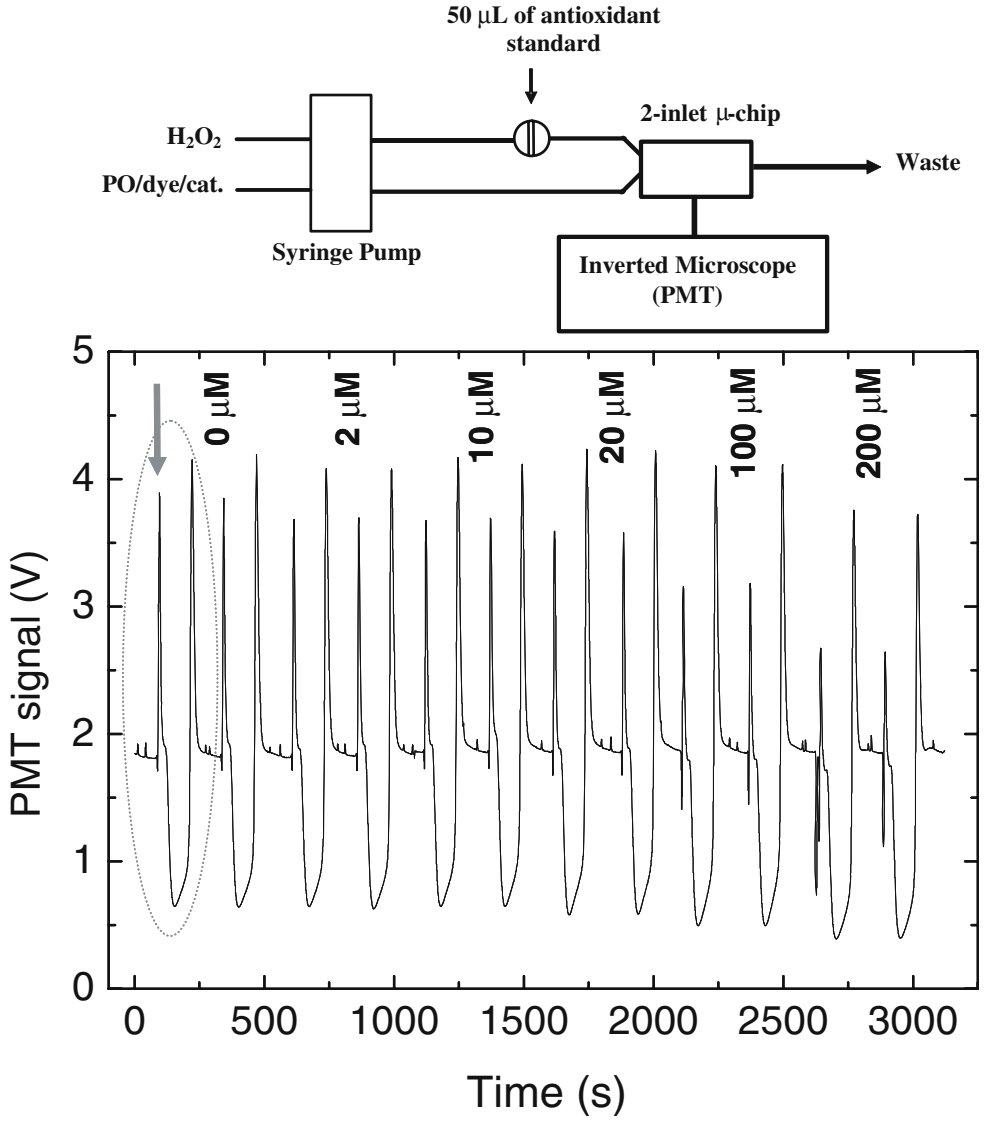

Fig. 6 Examples of the signal profiles obtained from the two-inlet microchip after duplicate injections of 0 to 200 μmol L^{-1} α-tocopherol antioxidant plugs (plug volume 50 μL). The *circled area* corresponds to a signal set resulting from a single injection and the *arrow* marks the peak used for quantitation

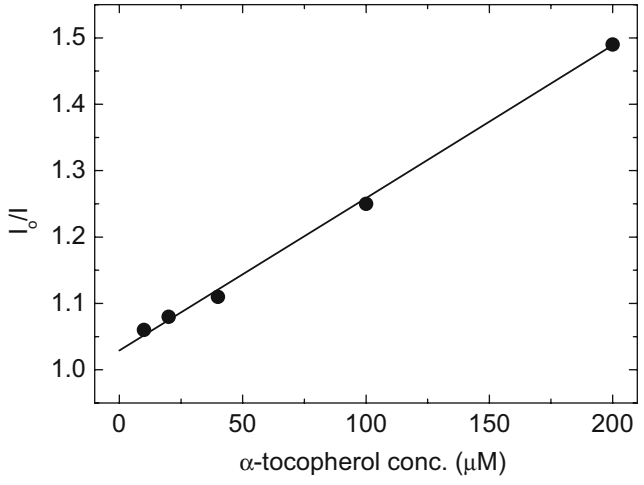

Fig. 7 Relationship between I_0/I and the concentration of α-tocopherol as obtained from the set of first positive peaks from Fig. 6. Calculation for the plot was performed using peak height

Table 1 Analytical performance of antioxidant assays using two-inlet microfluidic device

	β-carotene	α-tocopherol	quercetin
working range (μmol L^{-1})	2–200	10–200	50–100
calibration equation	y=0.0031x +1.05	y=0.0023x +1.02	y=0.0003x +1.04
correlation coefficient	0.9904	0.9969	0.9907
[a]precision (RSD), n=3	0.72	0.46	1.53
[b]limit of detection (μmol L^{-1})	1.92	9.92	48.08
[c]SA_{HP} ($\times 10^{-3}$ μmol^{-1} L)	3.27	2.36	0.31

[a] Calculated from the signal of 10 μM of β-carotene and α-tocopherol and 50 μM of quercetin.
[b] Calculated from 3σ (n=7) of the signals from the lowest concentration of each working range.
[c] Calculated form the calibration equation.

into a flowing reagent stream followed by diffusion and dispersion-based mixing and detection after a fixed time [35, 36]. Unlike most FIA-based methods, however, we use planar microchannels instead of capillaries or tubing; this enables potentially faster mixing [37] and also facilitates planar integration of optical detection components, for example organic photodetectors, to create fully portable systems for in-the-field use [31].

Finally the analytical performance of the two-inlet microfluidic device was assessed; the results are summarized in Table 1. Linearity calibrations were performed for all three antioxidants. The precision of the device is excellent (%RSD<2) for 50-μL injections (n=3) of 10 μmol L^{-1} β-carotene or α-tocopherol and 50 μmol L^{-1} quercetin. Detection limits (3σ) are at low micromolar levels. The capacity of antioxidants to scavenge hydrogen peroxide was calculated from the calibration equation and quoted as SA_{HP}. β-carotene was the most efficient hydrogen peroxide scavenger (SA_{HP} 3.27×10^{-3} μmol^{-1} L), followed by α-tocopherol (SA_{HP} 2.36×10^{-3} μmol^{-1} L) and quercetin (SA_{HP} 0.31×10^{-3} μmol^{-1} L).

This high hydrogen peroxide-scavenging efficiency of β-carotene is in good agreement with data published by Arnous et al., obtained with a cuvette based system [18], validating our microchip based PO-CL approach. It should be noted, however, that comparison of absolute SA_{HP} values is not possible, because different solvent systems were used, which greatly affects the solubility of lipophilic compounds such as β-carotene [5, 33]. This method is, instead, ideally suited to providing a ranking order of antioxidants, which would be invaluable for evaluation of a series of food sources or pharmaceutical supplements.

Conclusions

For the first time we have demonstrated a microfluidic system for estimation of antioxidant scavenging capacity. Detection is based on a modification of a previous cuvette-based PO-CL method with 9,10-bis(phenylethynyl)anthracene (BPEA) as a novel fluorophore. The microfluidic device was fabricated using standard PDMS rapid prototyping methods. Permanent plasma-based bonding of the microfluidic layer was used to enable operation at high flow rates with the organic solvents required for the antioxidant capacity assay. Controlled injection of antioxidant plugs was achieved through an injection valve, greatly enhancing assay sensitivity and response times. Further sensitivity and throughput improvements would be afforded by injecting smaller antioxidant plugs through on-chip injection schemes and optimization of the microfluidic layout by use of narrower and deeper microchannels. Studies in our laboratories are currently focused on integrating thin-film organic photodiodes within planar microchannel substrates to yield highly-miniaturized and portable microfluidic devices [38]. These studies will be reported in a forthcoming publication. We believe that such portable automated devices should be well-suited to low-cost in-the-field antioxidant capacity screening of plant-sourced food and pharmaceutical supplements.

Acknowledgements The authors would like to thank Molecular Vision Ltd and the Post Graduate Education and Research Program in Chemistry (Thailand) for financial support. MA acknowledges a Staff Development Scholarship (Commission on Higher Education, Ministry of Education, Thailand) and a Royal Golden Jubilee Ph. D. scholarship (from the Thailand Research Fund).

References

1. Halliwell B, Gutteridge JMC (1998) Free radicals in biology and medicine. Clarendon Press, Oxford, UK
2. Packer L, Hiramatsu M, Yoshikawa T (eds) (1999) Antioxidant food supplements in human health. Academic Press, London, UK
3. Huang DJ, Ou BX, Prior RL (2005) J Agric Food Chem 53:1841–1856
4. Miller NJ, RiceEvans CA (1997) Food Chem 60:331–337
5. van den Berg R, Haenen G, van den Berg H, Bast A (1999) Food Chem 66:511–517
6. Garcia-Alonso M, de Pascual-Teresa S, Santos-Buelga C, Rivas-Gonzalo JC (2004) Food Chem 84:13–18
7. Ivekovic D, Milardovic S, Roboz M, Grabaric BS (2005) Analyst 130:708–714
8. Wang H, Cao GH, Prior RL (1996) J Agric Food Chem 44:701–705
9. Cao GH, Sofic E, Prior RL (1996) J Agric Food Chem 44:3426–3431
10. Honer K, Cervellati R (2002) Eur Food Res Technol 215:437–442
11. Sun J, Chu YF, Wu XZ, Liu RH (2002) J Agric Food Chem 50:7449–7454
12. Ashida S, Okazaki S, Tsuzuki W, Suzuki T (1991) Anal Sci 7:93–96
13. Robinson EE, Maxwell SRJ, Thorpe GHG (1997) Free Radical Res 26:291–302
14. Bastos EL, Romoff P, Eckert CR, Baader WJ (2003) J Agric Food Chem 51:7481–7488
15. Cheng ZY, Yan GT, Li YZ, Chang WB (2003) Anal Bioanal Chem 375:376–380
16. Girotti S, Ferri E, Maccagnani L, Budini R, Bianchi G (2002) Talanta 56:407–414
17. Girotti S, Ferri E, Fini F, Bolelli L, Sabatini AG, Budini R, Sichertova D (2004) Talanta 64:665–670
18. Arnous A, Petrakis C, Makris DP, Kefalas P (2002) J Pharm Toxicol Methods 48:171–177
19. Mansouri A, Makris DP, Kefalas P (2005) J Pharm Biomed Anal 39:22–26
20. Chandross EA (1963) Tetrahedron Lett 4:761–765
21. Campbell AK (1988) Chemiluminescence. VCH, New York
22. Mohan AG, Burr JG (eds) (1985) Marcel Dekker, New York, pp 245–258
23. Sigvardson KW, Kennish JM, Birks JW (1984) Anal Chem 56:1096–1102
24. Rauhut MM, Roberts BG, Semsel AM (1966) J Am Chem Soc 88:3604–3617

25. Rauhut MM, Bollyky LJ, Roberts BG, Loy M, Whitman RH, Innotta AV, Semsel AM, Clark RA (1967) J Am Chem Soc 89:6515–6522
26. Jakeway SC, de Mello AJ, Russell EL (2000) Fresenius J Anal Chem 366:525–539
27. Reyes DR, Iossifidis D, Auroux PA, Manz A (2002) Anal Chem 74:2623–2636
28. Auroux PA, Iossifidis D, Reyes DR, Manz A (2002) Anal Chem 74:2637–2652
29. Verpoorte E (2002) Electrophoresis 23:677–712
30. Duffy DC, McDonald JC, Schueller OJA, Whitesides GM (1998) Anal Chem 70:4974–4984
31. Hofmann O, Miller P, Sullivan P, Jones TS, deMello JC, Bradley DDC, deMello AJ (2005) Sens Actuators B 106:878–884
32. Shamsipur M, Chaichi MJ (2003) J Photochem Photobiol A 155:69–72
33. Frankel EN, Meyer AS (2000) J Sci Food Agric 80:1925–1941
34. Squires TM, Quake SR (2005) Rev Modern Phys 77:977–1026
35. Ruzicka J, Hansen EH (2000) Anal Chem 72:212A–217A
36. Chen Y, Ruzicka J (2004) Analyst 129:597–601
37. Kamidate T, Kaide T, Tani H, Makino E, Shibata T (2001) Anal Sci 17:951–955
38. Wang X, Hofmann O, Das R, Barrett EM, deMello AJ, deMello JC, Bradley DDC (2006) Lab Chip. DOI 10.1039/b611067c